Journal of Medicinal Chemistry Article

J. Med. Chem. **2010,** *53,* 2433–2442 **2433**
DOI: 10.1021/jm901388c

Identification of 2-Anilino-9-methoxy-5,7-dihydro-6*H*-pyrimido[5,4-*d*][1]benzazepin-6-ones as Dual PLK1/VEGF-R2 Kinase Inhibitor Chemotypes by Structure-Based Lead Generation

Anne-Marie Egert-Schmidt,[†] Jan Dreher,[†] Ute Dunkel,[†] Simone Kohfeld,[†] Lutz Preu,[†] Holger Weber,[‡] Jan E. Ehlert,[‡] Bettina Mutschler,[‡] Frank Totzke,[‡] Christoph Schächtele,[‡] Michael H. G. Kubbutat,[‡] Knut Baumann,[†] and Conrad Kunick*[,†]

[†]*Technische Universität Braunschweig, Institut für Pharmazeutische Chemie, Beethovenstrasse 55, 38106 Braunschweig, Germany, and* [‡]*ProQinase GmbH, Breisacher Strasse 117, 79106 Freiburg, Germany*

Received September 18, 2009

To develop multikinase inhibitors with dual PLK1/VEGF-R2 inhibitory activity, the *d*-annulated 1-benzazepin-2-one scaffold present in the paullone family of kinase inhibitors was investigated as a general structure template suitable for anchoring annulated heterocycles at the hinge region of the ATP binding site. For this purpose, the indole substructure of the paullones was replaced by other nitrogen containing heteroaromatics. The designed scaffolds were synthesized and tested on the indicated kinases. The 2-anilino-5,7-dihydro-6*H*-pyrimido[5,4-*d*][1]benzazepin-6-ones were found to be VEGF-R2 inhibitors with selectivity against the insulin receptor kinase. The attachment of a methoxy group to the 9-position of the scaffold led to additional PLK1 inhibitory activity, which was explained by an alternative binding mode of the 9-methoxy derivatives. Selected members of the compound class inhibited the VEGF-R2 autophosphorylation in human umbilical vein endothelial cells, the sprouting of human umbilical vein endothelial cell speroids, and the proliferation of diverse cancer cell lines.

Introduction

Because overexpression and hyperactivity of protein kinases is frequently observed in human tumor tissues, the inhibition of certain protein kinases was established as a therapeutic concept during the past decade.[1−3] In the beginning of the protein kinase inhibitor era, the selective inhibition of only one target enzyme appeared desirable to limit unwanted side effects. However, given the high similarity of the ATP-binding pocket architecture in the protein kinases and the fact that besides a few exceptions[4] the majority of established kinase inhibitors compete with ATP at the ATP-binding site of the enzyme, it is not surprising that most kinase inhibitors show a modest degree of protein kinase selectivity. Hitting more than one tumor-related protein kinase at a time is not necessarily a drawback but offers the advantage of a broader application of the drug against diverse tumor entities on the one hand and a lower risk of drug-resistance development during treatment on the other hand.[5] Recently multikinase inhibitors have been launched as anticancer drugs, e.g., sunitinib,[6] sorafenib,[7] and dasatinib.[8,9]

The investigation reported here was directed to find dual inhibitors of the tumor-related kinases polo-like kinase 1 (PLK1[a]) and VEGF-R2 (vascular endothelial growth factor-receptor 2).

PLK1 is an important serine/threonine kinase necessary for cell division and tissue proliferation of eukaryotes. During mitosis, PLK1 regulates centrosome maturation, microtubule-kinetochore attachment, and the onset of cytokinesis during late mitosis. During anaphase, PLK1 initiates cleavage furrow ingression and spindle elongation. Cells treated with PLK inhibitors fail to divide and exit mitosis as tetraploid binucleates.[10] PLK1 is overexpressed in a variety of human cancer tissues and high PLK1 levels are correlated with poor prognosis.[11] PLK1-depletion by siRNA is able to induce apoptosis,[12] and inhibition of PLK1 by antisense-oligonucleotides resulted in growth inhibition of cancer cells.[13] Furthermore, application of short hairpin RNA against PLK1 resulted in cancer inhibition in a nude mice model.[14] In murine xenograft assays, the potent ATP-competitive and selective synthetic PLK1-inhibitor BI2536 also inhibited tumor growth.[15] Taken together, these findings lead to the suggestion that PLK1 is a valid biological target for potential anticancer therapeutics.[11]

The inhibition of tyrosine kinase receptors of the vascular endothelial growth factor (VEGF) is one of the main modes of action of the mentioned multikinase inhibitors sunitinib[16,17] and sorafenib.[7] To grow beyond a volume of 1−2 mm^3, a solid tumor depends on the supply of the cancer cells with oxygen and nutrients through blood vessels.[18] For an induction of

*To whom correspondence should be addressed. Phone: +49-531-391-2754. Fax: +49-531-391-2799. E-mail: c.kunick@tu-braunschweig.de.

[a] Abbreviations: ACN, acetonitrile; AcOH, acetic acid; ATP, adenosine triphosphate; AUC, area under curve; CDK, cyclin dependent kinase; CK1, casein kinase 1; DAD, diode array detector; DCM, dichloromethane; DMF, *N*,*N*-dimethyl formamide; DMF-DMA, dimethylformamide dimethyl acetal; DMSO, dimethyl sulfoxide; DTT, dithiothreitol; EGF, epidermal growth factor; EtOH, ethanol; gk, gatekeeper; GSK-3, glycogen synthase kinase-3; HEPES, *N*-2-hydroxyethylpiperazine-*N*′-2-ethanesulfonic acid; HPLC, high performance liquid chromatography; HUE, human umbilical endothelial (cells); HUVEC, primary human umbilical vein endothelial cells; INS-R, insulin receptor kinase; IVCLS, in vitro cell line screening; NCI, National Cancer Institute; PCC, pairwise correlation coefficient; PDB, Protein Data Bank; PEG, polyethylene glycol; PFK, perfluorokerosene; PLK1, polo-like kinase 1; RPMI, Roswell Park Memorial Institute; SRB, sulforhodamine B; TCA, trichloroacetic acid; TFA, trifluoroacetic acid; TLC, thin layer chromatography; TMB, 3,3′,5,5′-tetramethylbenzidine; VEGF-R, vascular endothelium growth factor receptor kinase.

Published on Web 02/19/2010

Chart 1. Structures of Paullones: Kenpaullone (**1**), Alsterpaullone (**2**), 1-Azakenpaullone (**3**), and 2-Azakenpaullone (**4**)

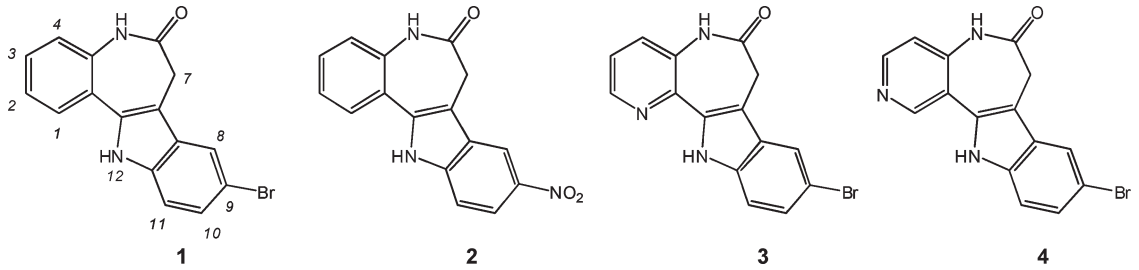

angiogenesis, the tumor secrets VEGF and other growth factors which interact with VEGF receptors (VEGF-Rs) on vascular endothelial cells (ECs). The ECs then escape from the existing blood vessel walls and proliferate toward the source of the VEGF. After formation of new tubular structures, blood flows through the new capillaries. The uncontrolled angiogenesis in tumor tissue is characterized by an irregular and chaotic structure of the blood vessels. A high vascularization is not only a prerequisite for growth of solid tumors but also increases the formation of metastases. Within the VEGF receptor family, VEGF-R1 (Flt1) is involved in the early inflammation process by regulation of monocyte and macrophage chemotaxis. VEGF-R3 (Flt4) is important for lymphangiogenesis and thus may play a role in the dissemination of lymphatic metastases of solid tumors. Located on endothelial cells (ECs), VEGF-R2 (KDR) is responsible for tumor angiogenesis. The inhibition of VEGF-R kinases located on ECs bears the advantage that in contrast to the tumor cells the ECs are genetically stable and therefore less prone to develop resistance against antiproliferative agents. VEGF-R2 is one of the crucial target structures of the mentioned multikinase inhibitors sorafenib and sunitinib as well as of drugs currently in clinical development.[19−21] We hypothesized that a single agent inhibiting both PLK1 and VEGF-R2 might interfere with tumor growth both on the level of uncontrolled cell division and tumor vascularization. We therefore were interested to find novel chemotypes with such dual kinase inhibition profiles as starting points for an anticancer drug development campaign.

For the rational idea-generation toward novel protein kinase inhibitor lead structures, it has been suggested to use the structural data of protein kinase−ligand complexes in the Protein Data Bank (PDB).[22] A recent analysis of the available PDB files of protein kinases cocrystallized with diverse inhibitors identified 53 molecular inhibitor substructures that are responsible for binding to the hinge region in the ATP-binding pocket of kinases.[22] The main binding feature of these structure motifs is a pattern of one to three hydrogen bonds between the inhibitor and three attachment points in the hinge segment of the protein kinase, namely the backbone carbonyl oxygen of the amino acid next to the "gatekeeper" residue (gk+1) and both backbone carbonyl and NH group of the amino acids two positions toward the carboxy terminus, the so-called "gk+3" amino acid.[22]

We here report a search for dual PLK1/VEGF-R2 inhibitor chemotypes comprising the *d*-annulated 1,3-dihydro-2*H*-1-benzazepin-2-one scaffold present in the paullone kinase inhibitor structure. Because the paullone basic structure was not included in the compilation of characteristic ATP pocket-binding motifs published by Ghose at al.,[22] we intended to generate protein kinase inhibitors with a certain degree of novelty by this method.

The paullones (Chart 1) represent a group of established inhibitors of cyclin-dependent kinases (CDKs) and glycogen synthase kinase-3 (GSK-3).[23] Among this compound class, kenpaullone (**1**) is a commercially available dual CDK/GSK-3-inhibitor.[24] Kenpaullone's 9-nitro analogue, alsterpaullone (**2**), displays enhanced CDK/GSK-3 inhibitory potency and induces apoptosis in cancer cells by perturbation of the mitochondrial inner membrane potential.[25] The binding mode of alsterpaullone to the ATP binding pocket of GSK-3β was elucidated by X-ray structure analysis of a protein−ligand complex (PDB entry 1Q3W).[26] Alsterpaullone binds, among others, by two direct hydrogen bonds emanating from the lactam moiety directly to the gk+3 amino acid. A third water mediated hydrogen bond connects the lactam carbonyl to the gk+1 amino acid carbonyl group.[26] While the commercially available 1-aza-kenpaullone (**3**) is widely used as selective GSK-3 inhibitor,[27] its 2-aza isomer **4** lacks selectivity, showing dual CDK/GSK-3 inhibitory activity similar to kenpaullone **1**.[28] In a panel of 71 protein kinases, 1 μM concentrations of kenpaullone inhibited 9 other kinases besides GSK3 and CDK2/cyclin A.[29] This observation suggests that the benzolactam motif of the paullones might be a general hinge-binding element. Using this information, we designed the potential protein kinase inhibitor chemotypes A−D (Table 1) by replacing the indole ring of the paullones by other heterocyclic systems. The particular structures were chosen because a straightforward synthesis procedure from simple common heterocyclic enaminones was envisaged for these scaffolds.

A preliminary docking study was carried out to check whether prototypes **21**, **24a**, and **28a** of the designed inhibitors might fit in the ATP binding pockets of the mentioned target kinases. The insulin receptor kinase (INS-R) was included in these studies as a counter kinase of indispensable physiological importance. It was explicitly desired that the newly developed kinase inhibitors should not affect INS-R in order to prevent diabetes mellitus-like side effects during a possible therapeutic use of the compounds. The docking placed the designed inhibitors into the ATP binding sites of VEGF-R2 and PLK1 in meaningful poses, albeit **28a** was oriented toward the hinge area of the kinases not with its benzolactam element but by the anilinopyrimidine partial structure. **21** and **24** were only partially accommodated in the INS-R ATP binding site suggesting that a selectivity toward this kinase was conceivable. These preliminary results warranted the synthesis of the designed compounds in order to evaluate both their VEGF-R2/PLK1 inhibitory activity and their selectivity against INS-R.

Chemistry

The test compounds listed in Table 1 were synthesized from suitable enaminones **9**, **10**, **11**, or **12**, respectively, which were

Table 1. Structures and Kinase Inhibitory Activity of *d*-Annulated Benzazepinones

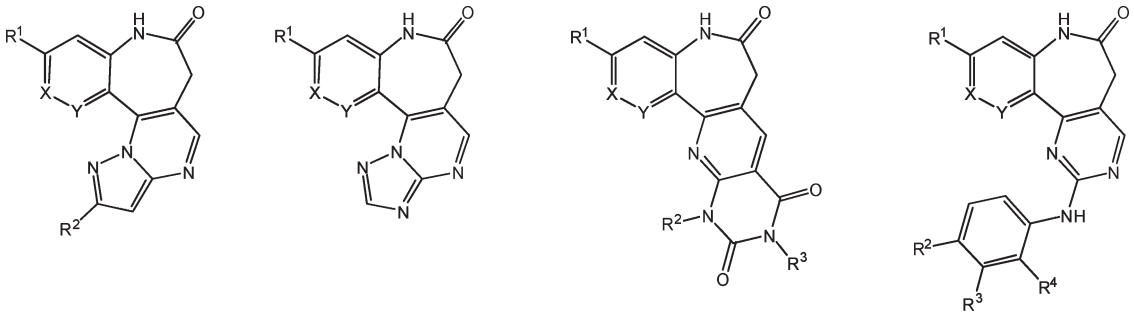

A B C D

code	basic structure	X	Y	R^1	R^2	R^3	R^4	IC_{50} VEGF-R2 [μM]	IC_{50} PLK1 [μM]	IC_{50} INS-R [μM]
1[a]								> 100[a]	> 100[a]	> 100[a]
17a	A	CH	CH	H	H			12	> 100	> 100
17b	A	CH	CH	H	−Ph			0.63	> 100	> 100
18a	A	CH	CH	$-OCH_3$	H			8.6	> 100	> 100
18b	A	CH	CH	$-OCH_3$	−Ph			1.8	17	11
19	A	N	CH	H	−Ph			2.0	> 100	> 100
20a	A	CH	N	H	H			87	> 100	> 100
20b	A	CH	N	H	−Ph			16	> 100	> 100
21	B	CH	CH	H				NI[b]	NI[b]	NI[b]
22	B	CH	CH	$-OCH_3$				> 100	> 100	> 100
23	B	CH	N	H				> 100	> 100	> 100
24a	C	CH	CH	H	H	H		> 100	> 100	> 100
24b	C	CH	CH	H	CH_3	CH_3		> 100	> 100	> 100
25a	C	CH	CH	$-OCH_3$	H	H		> 100	> 100	> 100
25b	C	CH	CH	$-OCH_3$	CH_3	CH_3		> 100	> 100	> 100
26a	C	N	CH	H	H	H		> 100	> 100	> 100
26b	C	N	CH	H	CH_3	CH_3		> 100	> 100	> 100
27a	C	CH	N	H	H	H		66	> 100	> 100
27b	C	CH	N	H	CH_3	CH_3		> 100	> 100	> 100
28a	D	CH	CH	H	H	H	H	0.14	> 100	> 100
28b	D	CH	CH	H	I	H	H	0.4	15	> 100
28c	D	CH	CH	H	$-OCH_3$	H	H	0.095	47	99
28d	D	CH	CH	H	Cl	H	H	0.19	> 100	> 100
28e	D	CH	CH	H	$-NO_2$	H	H	0.33	> 100	22
28f	D	CH	CH	H	$-CH_3$	H	H	0.19	> 100	> 100
28g	D	CH	CH	H	−OH	H	H	0.08	> 100	> 100
28h	D	CH	CH	H	Br	H	H	0.29	> 100	> 100
28i	D	CH	CH	H	$-OC_2H_5$	H	H	0.13	> 100	> 100
28j	D	CH	CH	H	H	−OH	H	0.051	19	> 100
28k	D	CH	CH	H	H	H	Cl	6.1	73	> 100
28l	D	CH	CH	H	H	H	Br	57	> 100	> 100
28m	D	CH	CH	H	H	H	−OH	0.53	14	> 100
28n	D	CH	CH	H	$-OCH_3$	−OH	H	0.073	5.7	24
28o	D	CH	CH	H	−OH	−Cl	H	0.035	9.3	84
28p	D	CH	CH	H	−OH	H	CH_3	1.2	20	> 100
29g	D	CH	CH	$-OCH_3$	−OH	H	H	0.028	0.75	> 100
29c	D	CH	CH	$-OCH_3$	$-OCH_3$	H	H	0.050	0.35	> 100
29i	D	CH	CH	$-OCH_3$	$-OC_2H_5$	H	H	0.052	7.3	> 100
29j	D	CH	CH	$-OCH_3$	H	−OH	H	0.015	0.84	> 100
29n	D	CH	CH	$-OCH_3$	$-OCH_3$	−OH	H	0.018	0.14	> 100
29o	D	CH	CH	$-OCH_3$	−OH	−Cl	H	0.011	0.36	> 100
30g	D	N	CH	H	−OH	H	H	0.13	2.6	> 100
30c	D	N	CH	H	$-OCH_3$	H	H	0.19	2.5	> 100
30i	D	N	CH	H	$-OC_2H_5$	H	H	0.099	1.7	> 100
30j	D	N	CH	H	H	−OH	H	0.14	2.3	> 100
30o	D	N	CH	H	−OH	−Cl	H	0.087	1.4	> 100
31g	D	CH	N	H	−OH	H	H	2.7	55	> 100
31c	D	CH	N	H	$-OCH_3$	H	H	1.5	> 100	> 100
31i	D	CH	N	H	$-OC_2H_5$	H	H	2.0	> 100	> 100
31j	D	CH	N	H	H	−OH	H	2.6	> 100	> 100
31o	D	CH	N	H	−OH	−Cl	H	0.67	> 100	> 100

[a] The IC_{50} values for kenpaullone were determined in the presence of 0.1 μM ATP. For all other compounds except kenpaullone the ATP concentration was 1 μM. [b] NI = not inhibited (less than 30% inhibition @ 10 μM concentration of **21**).

Scheme 1. Synthesis of *d*-Annulated Benzazepinones and Azaanalogues[a]

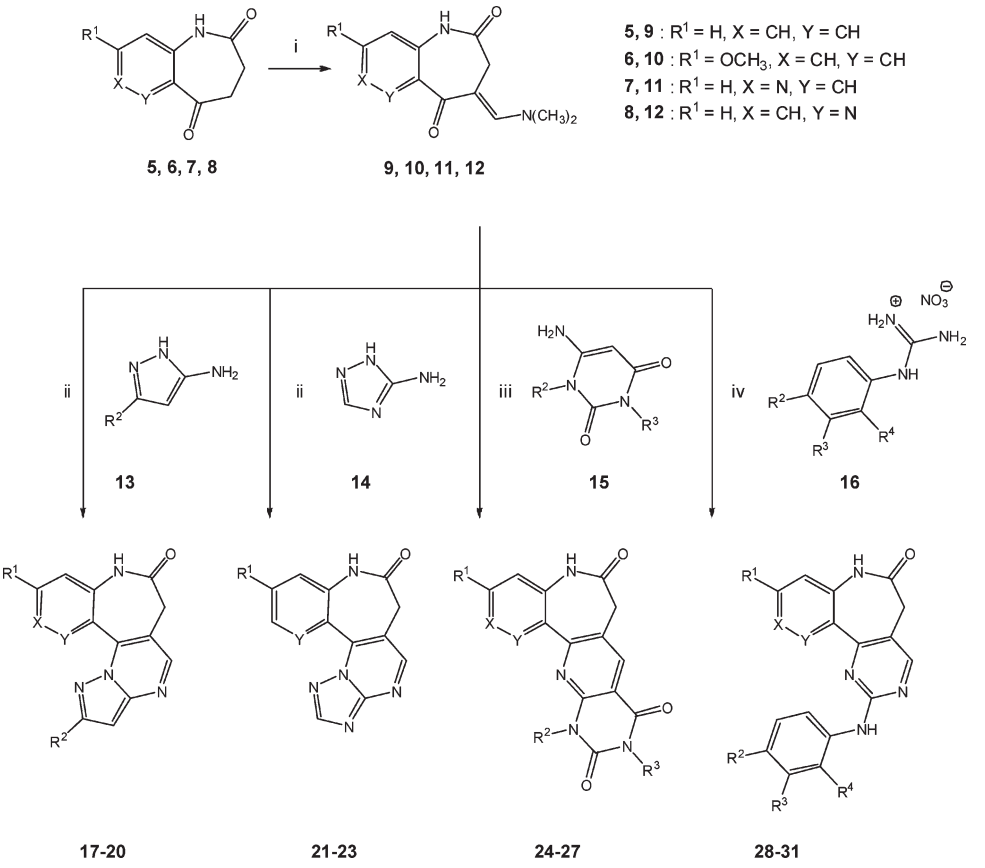

[a] (i) DMF-DMA, 115 °C, 2.5 h; (ii) AcOH, 120−140 °C (microwave oven), 10 min; (iii) AcOH, reflux, 4−12 h; (iv) NaOH, propan-2-ol, reflux, 8 h or 150 °C (microwave oven), 30−40 min.

readily prepared from the cyclic precursor ketones **5**,[30] **6**,[31] **7**,[28] or **8**[27] by reaction with dimethylformamide dimethylacetal (DMF-DMA) using a method originally described for the synthesis of **9** from the oxolactam **5**.[32]

Heating the enaminones **9**−**12** with 1*H*-pyrazol-5-amines **13** in glacial acetic acid in a single mode microwave device afforded the annulated pyrazolopyrimidines **17**−**20** in moderate to good yields. In a similar procedure, the annulated triazolopyrimidines **21**−**23** were obtained using 3-amino-1*H*-1,2,4-triazole (**14**) as dinucleophile. The annulated pyrimidopyridines **24**−**27** were obtained by refluxing the enaminones **9**−**12** with 6-aminouracil derivatives **15** in acetic acid. For the synthesis of the anilinopyrimidines **28**−**31**, the arylguanidinium nitrates **16** were heated with the enaminones **9**−**12** in the presence of sodium hydroxide in propan-2-ol either under conventional conditions or in a microwave device, yielding the products **28**−**31** in modest (17%; **29n**) to good yields (77%, **28g**) (Scheme 1).

Biological Evaluation and Discussion

The compounds listed in Table 1 were evaluated in vitro by measuring the IC_{50} values on VEGF-R2, PLK1, and INS-R in a radiometric protein kinase assay (^{33}PanQinase activity assay). The results revealed that the new *d*-annulated compounds **21**−**23** (scaffold B) and **24**−**27** (scaffold C) were devoid of noteworthy activity against the three kinases. Considering the results of the docking studies, these results were not surprising with regard to INS-R but were disappointing with regard to VEGF-R2 and PLK1. Exchange of the nitrogen in position 3 of the prototype B for a carbon atom leads to prototype A. Interestingly, all members of this subgroup of compounds (**17**−**19**) exhibited a considerable inhibition of VEGF-R2. At this time, we have no reasonable explanation for the different VEGF-R2 inhibitory activity of scaffolds A and B. None of the derivatives belonging to scaffolds A−C was further pursued because either the PLK1 kinase remained unaffected or, as was found for **18b**, the INS-R counter kinase was inhibited as well.

In contrast to the results with the aforementioned compounds, virtually all derivatives based on the parent scaffold D showed potent kinase inhibitory activity for VEGF-R2. However, most of the structures **28** with the plain benzo annulation do not show the intended dual-kinase inhibition. Only the 3′,4′-disubstituted derivatives **28n** and **28o** exhibit at least one-digit micromolar inhibition concentration for PLK1. The derivatives **28k**,**l**,**m**,**p** displaying a 2′-substitution at the phenyl group showed the lowest activity toward VEGF-R2 within this subgroup. Interestingly, the placement of a 9-methoxy-group into the parent scaffold D (compound class **29**) improved the PLK1 inhibitory activity by at least 1 order of magnitude. Fortunately, none of these 9-methoxy derivatives **29** inhibited the counter-kinase INS-R. A replacement of the annulated benzene ring for a pyrido substructure led to different results depending on the position of the pyrido nitrogen. The derivatives **30**, displaying the pyrido nitrogen in 10-position, exhibited kinase inhibitory activity comparable to the benzo analogues **28**. In contrast, upon introduction of a nitrogen in position 11 (Y = N; compounds **31**, refer to Table 1), the VEGF-R2 inhibitory activity was strongly

Table 2. Cellular Bioactivity of Selected "Anilinopyrimidines" D

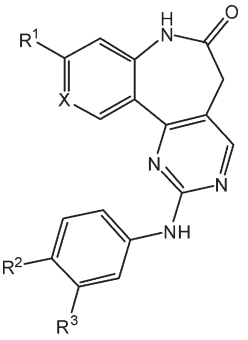

D

code	basic structure	X	R^1	R^2	R^3	inhibition of VEGF-R2 phosphorylation in HUE cells [IC_{50}, μM]	inhibition of HUVEC sprouting [IC_{50}, μM]
28j	D	CH	H	H	−OH	1.6	NT[a]
28n	D	CH	H	$-OCH_3$	−OH	2.4	NT[a]
28o	D	CH	H	−OH	−Cl	9.6	NT[a]
29i	D	CH	$-OCH_3$	$-OC_2H_5$	H	0.29	1.1
29o	D	CH	$-OCH_3$	−OH	−Cl	0.43	1.2
30i	D	N	H	$-OC_2H_5$	H	18.6	NT[a]
30o	D	N	H	−OH	−Cl	NI[b]	NT[a]
staurosporine[c]						0.07	

[a] NT = not tested. [b] NI = not inhibited at 10 μM inhibitor concentration. [c] Staurosporine was used as a positive control.

diminished and the PLK1-inhibition was lost completely. At the present stage, we have no satisfactory explanation for the different kinase inhibitory activity of **30** and **31** on a molecular basis.

To investigate whether the new compounds are also able to cross membranes and display kinase inhibitory activity in a cellular environment, seven selected derivatives were studied in cellular phosporylation assays. For these studies, human umbilical endothelial (HUE) cells were treated with the compounds and then stimulated by VEGF. As readout, the autophosphorylation of VEGF-R2 was determined. The important role of the positions 9 and 10 of the parent ring system for the cellular bioactivity can be clearly demonstrated by the comparison of **28o**, **29o**, and **30o**. All three congeners have the same substitution pattern at the phenyl substituent and inhibit the isolated VEGF-R2 enzyme in two-digit nanomolar concentrations. However, while for inhibition of VEGF-R2 in HUE cells high concentrations (9.6 μM) of **28o** are necessary and the pyrido derivative **30o** is not active up to 10 μM, the 9-methoxy congener **29o** inhibits the cellular kinase in submicromolar concentrations (0.43 μM). The 9-methoxy derivative **29i** proved to be even more potent in the cellular experiment. As a result of these findings, the impact of **29i** and **29o** on endothelial cell sprouting was studied in spheroid-based cellular angiogenesis assays. In these investigations, spheroids of human umbilical vein endothelial cells (HUVEC) cultured in collagen were treated concomitantly with VEGF and the test compounds. Both **29i** and **29o** showed a clear inhibition of the sprout growths from the spheroids after 24 h incubation in low micromolar concentrations (EC_{50} = 1.1 and 1.2 μM, respectively, refer to Table 2). These results are promising regarding a potential use of this compound class to suppress angiogenesis in tumor tissue.

For a preliminary evaluation of the antiproliferative activity of the new kinase inhibitors, seven representatives of the structure families **28**, **29**, and **30** were tested in the in vitro cell line screening (IVCLS)[33] of the National Cancer Institute for growth inhibition on 60 human tumor cell lines. While all compounds exhibited a strong antiproliferative activity, a characteristic selectivity pattern was observed for distinct cell lines. For example, some cell lines from the renal cancer subpanel (e.g., CAKI-1) were especially sensitive to the growth inhibitory activity of the compounds. Furthermore, a characteristic selectivity pattern was found within certain subpanels. For instance, the ovarian cancer cell line IGROV1 typically was stronger inhibited than other cell lines from the same subpanel. In contrast, the cell line UACC-257 proved to be rather resistant against the tested derivatives, with concentrations needed to inhibit this melanoma-derived tumor cells being 2 orders of magnitude higher than for the cell lines mentioned before (Table 3).

A pronounced selectivity in the IVCLS is regarded as an indicator of a specific biological mechanism addressing distinct biological targets. For the structures presented here, it is assumed that inhibition of a set of cancer-related protein kinases contributes to growth inhibition. If this was the case, the IVCLS selectivity pattern of the studied compounds should show a considerable degree of similarity. Such similarity of patterns can be studied and quantified by the COMPARE[34,35] computer tool which is accessible via the NCI's Developmental Therapeutics Program Web site.[36] For two compounds tested in the IVCLS, COMPARE calculates a pairwise correlation coefficient (PCC) as an index of similarity. The maximal PCC value is 1, indicating that the compared patterns are completely identical. A number of results from

Table 3. Antiproliferative Activity of Selected Anilinopyrimidines D on Tumor Cell Lines in the in Vitro Cell Line Screening of the National Cancer Institute

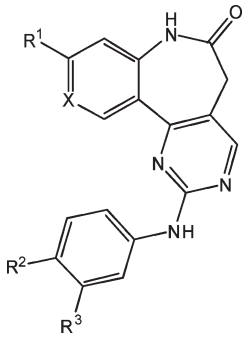

D

						GI_{50} [μM][a]		
code	basic structure	X	R^1	R^2	R^3	IGROV1[b]	CAKI-1[c]	UACC-257[d]
28c	D	CH	H	$-OCH_3$	H	0.41	0.51	61
28g	D	CH	H	$-OH$	H	3.0	2.6	> 100
28i	D	CH	H	H	$-OH$	0.38	0.75	27
28n	D	CH	H	$-OCH_3$	$-OH$	0.25	0.15	19
28o	D	CH	H	$-OH$	$-Cl$	na[e]	4.7[f]	39[f]
29i	D	CH	$-OCH_3$	$-OC_2H_5$	H	0.23[f]	0.39	55
30i	D	N	H	$-OC_2H_5$	H	0.40	0.16[f]	> 100

[a] GI_{50} = concentration for 50% cell growth inhibition. If not indicated otherwise, results are averaged values from two independent test runs carried out at different dates. Each test run was carried out in duplicate. Maximum tested concentration was 100 μM. If the GI_{50} was above 100 μM, the maximum concentration was used for calculation of averaged values; [b] Ovarian cancer cell line. [c] Renal cancer cell line. [d] Melanoma cell line. [e] na = test value not available. [f] Single test run.

the literature demonstrate that COMPARE is suitable to identify activity mechanisms of antiproliferative compounds. While it has been suggested that correlations >0.6 indicate similar mechanisms within cells,[37] distinct structural compound families can be clustered by lower thresholds down to PCC's > 0.35.[38]

The results listed in Table 4 show a remarkable correlation, documented by high PCC's > 0.6, for all compounds **28** that were tested in the IVCLSP. The aza analogue **30i** also displayed a considerable correlation to this group of compounds. In contrast, the 9-methoxy analogue **29i** was clearly distinguished from the other compounds because not a single PCC value >0.6 was found. This observation is consistent with the finding that introduction of a 9-methoxy group produces a change in potency and kinase selectivity of the anilinopyrimidines belonging to parent scaffold D.

An interesting result of this study is the superiority of the compounds **29g**,**c**,**j**,**n**,**o** versus their counterparts from the series **28**, **30**, **31** regarding the inhibition of PLK1. While most of the latter derivatives were either not or only poor PLK1 inhibitors, the majority of the compounds **29** exhibited inhibitory activity in submicromolar concentrations. A pairwise comparison of structural analogues, e.g., of **28o** and **29o**, reveals a more than 20-fold improvement in PLK1 inhibitory activity by the introduction of the methoxy group into position 9 (**28** → **29**). Because of these large differences in biological activity, the binding modes of the compounds **29** to PLK1 were studied by molecular docking. A high-scored docking pose of **29n** in PLK1 is shown in Figure 1. Obviously, the 9-methoxy group of **29n** fits closely into a hydrophobic pocket formed by amino acids Gly62 and Ala65 at the "roof" of the ATP binding site.

Table 4. Matrix COMPARE of Compounds Tested in the in Vitro Cell Line Screening of the National Cancer Institute[a,b]

(a)

	28i	28c	28n	28o	28g	30i	29i
28i		0.863	0.791	0.864	0.79	0.614	0.399
28c	0.863		0.828	0.725	0.751	0.683	0.454
28n	0.791	0.828		0.73	0.607	0.641	0.397
28o	0.864	0.725	0.73		0.654	0.403	0.156
28g	0.79	0.751	0.607	0.654		0.578	0.489
30i	0.614	0.683	0.641	0.403	0.578		0.501
29i	0.399	0.454	0.397	0.156	0.489	0.501	

(b)

< 0.3	0.3 – 0.399	0.4 – 0.499	0.5 – 0.599	0.6 – 0.699	0.7 – 0.799	0.8 – 0.899

[a] (a) Color code for pairwise correlation coefficients calculated by the COMPARE algorithm. [b] (b) GI_{50} values were used. 49−59 cell lines were included in the calculation of the correlation coefficient.

To highlight the importance of the presence of the 9-methoxy group, a study of the interaction potential between a molecular probe and the binding pocket was carried out using the program GRID.[39] Using a methyl group as probe at

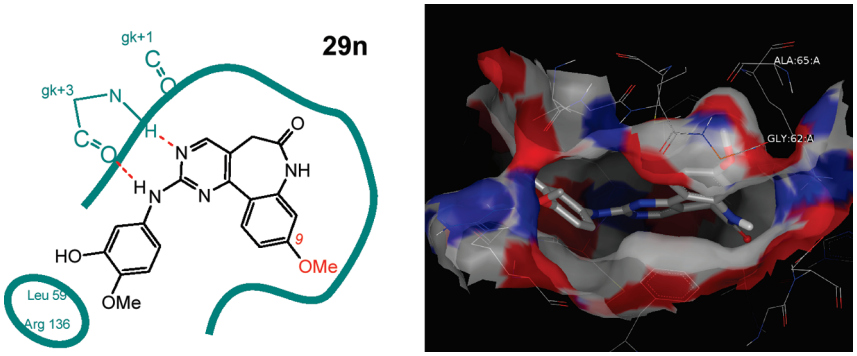

Figure 1. Docking pose of **29n** in the ATP-binding site of PLK1. Left, 2D sketch; right: 3D visualization. gk+1; gk+3, amino acid position related to the gatekeeper position in the hinge motif of the kinase. The 9-methoxy group of **29n** (red color in the 2D-drawing) fits into a pocket formed by the amino acids Gly62 and Ala65 (structures calculated by the docking module of the Schrödinger 2008 Suite; structure of the host molecule: PDB code 2OWB).

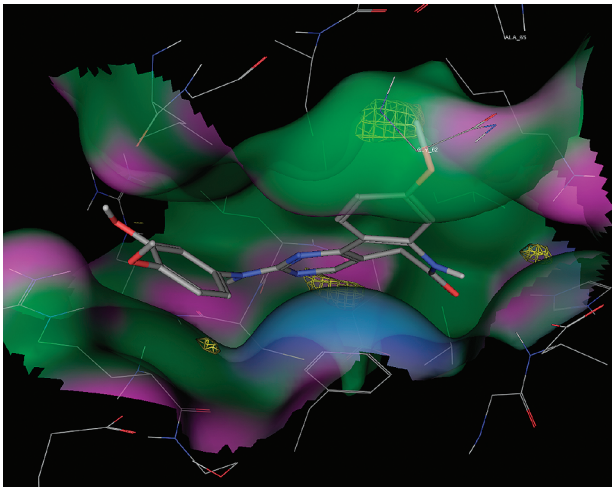

Figure 2. Hotspot analysis within the ATP binding site of PLK1 using a methyl probe identified the indicated pocket (yellow grid shape in the upper center of the picture) as area most contributing to positive ligand−protein interactions. The depicted bound structure **29n** is directing the 9-methoxy group into the identified hotspot area.

a contour level of −4 kcal/mol, the area accommodating the 9-methoxy group of **29n** was identified as a favorable binding region for hydrophobic parts of the ligand (see Figure 2).

A thorough literature survey revealed that recently congeners of the basic structure **28** have been filed as inhibitors of Aurora A and Aurora B kinase, Checkpoint kinase 1 (Chk-1), and PLK1.[40] However, the structural basis for the kinase inhibition by **28**, the concomitant inhibition of VEGF-R2 kinase and the activity of the compounds in cellular angiogenesis models has not yet been mentioned. Moreover, the major impact of the 9-methoxy group present in the novel derivatives **29** for kinase inhibitory activity has not been reported previously.

Future studies are directed to explore comprehensively the group of 9-methoxy-substituted derivatives **29** and to broadly check their protein kinase profiles and their antiproliferative activity in cancer cell lines. Further tests in additional cellular assays are necessary to determine which of the inhibited protein kinases are crucial for the observed antiproliferative activity in cancer cell lines.

Conclusion

On the basis of the starting hypothesis that the seven-membered lactam structure present in the paullone basic scaffold might serve as a suitable hinge-binder template for the design of dual VEGF-R2/PLK1 inhibitors, several new heterocyclic scaffolds were synthesized and screened. Among the designed structure classes, only 2-anilino-9-methoxy-5,7-dihydro-6*H*-pyrimido[5,4-*d*][1]-benzazepin-6-ones **29** display the desired dual potent VEGF-R2/PLK1 inhibitory activity. A docking study indicated the important role of the 9-methoxy group of **29** which fits into a pocket formed by the amino acids Gly62 and Ala65 in the ATP binding site of PLK1. Selected examples of the basic scaffolds **28** and **29** showed inhibition of VEGF-R2 autophosphorylation in cells, inhibitory activity in a cellular angiogenesis model, and antiproliferative activity on cancer cell lines in vitro.

Experimental Section

Kinase Assays. A radiometric protein kinase assay (^{33}PanQinase Activity Assay) was used for measuring the activity of the protein kinases. All assays were performed with a BeckmanCoulter/Sagian robotic system and 96-well FlashPlates from Perkin-Elmer/NEN (Boston, MA) in a 50 μL reaction volume. The reaction cocktail was pipetted in 4 steps in the following order: 20 μL of assay buffer, 5 μL of ATP solution (in H_2O), 5 μL of test compound (in 10% DMSO), 10 μL of substrate/10 μL of enzyme solution (premixed). The assay for all enzymes contained 60 mM HEPES-NaOH, pH 7.5, 3 mM $MgCl_2$, 3 mM $MnCl_2$, 3 μM Na-orthovanadate, 1.2 mM DTT, 50 μg/mL PEG_{20000}, 1 μM [γ-^{33}P]-ATP (approximately 5 × 10^5 cpm per well). The following substrates were used [substrate amount in square brackets given in ng/50 μL]: $Poly(Glu,Tyr)_{4:1}$ [125] for VEGF-R2, $Poly(Glu,Tyr)_{4:1}$ [125] or $Poly(Ala,Glu,Lys,Tyr)_{6:2.5:1}$ [125] for INS-R; RBER-CHKtide [2000], or Casein [1000] for PLK1. The reaction cocktails were incubated at 30 °C for 80 min. The reaction was stopped with 50 μL of 2% (v/v) H_3PO_4, and plates were aspirated and washed two times with 200 μL of 0.9% (w/v) NaCl. Incorporation of $^{33}P_i$ was determined with a microplate scintillation counter (Microbeta Trilux, Wallac). For calculation of IC_{50} values, data were generated for comparison without enzyme in the presence of substrate ("low control"). Moreover, data with enzyme but without inhibitor were generated ("high control"). The difference between high and low control was taken as 100% enzyme activity. The residual activities for each concentration and the compound IC_{50} values were calculated using Quattro Workflow V2.x (Quattro Research GmbH, Munich, Germany; www.quattroresearch.com). The fitting model for the IC_{50} determinations was "Sigmoidal response (variable slope)" with parameters "top" fixed at 100% and "bottom" at 0%. The fitting method used was a least-squares fit.

In case of solubility problems, outliers in the higher concentration range were removed to generate more realistic sigmoidal curves for IC_{50} calculation. Assays were carried out in singlicate. As parameter for assay quality, the Z'-factor[41] was calculated for the low and high controls of each plate. Assay plates were repeated in case the Z'-factor drops below 0.4.

Cellular VEGF-R2 Autophosphorylation Assays. In brief, spontaneously immortalized human umbilical vein endothelial (HUE) cells were seeded in 48-well culture plates in complete endothelial growth medium and after overnight attachment starved in the same medium devoid of growth supplement. On the day of the assay, cells were treated with test compounds for 90 min at a DMSO concentration of 1%, followed by stimulation of VEGF-R2 autophosphorylation using 100 ng/mL of ligand $VEGF_{165}$ for 3 min at room temperature. Subsequently, cells were lysed and lysates loaded onto a sandwich ELISA coated with anti-VEGFR2 antibody 3G2. The tyrosine phosphorylation status of bound VEGF-R2 was subsequently detected by biotinylated pY-99 antibody, which was then detected by horseradish peroxidase labeled streptavidin followed by a chromophoric reaction using TMB substrate. Absorption values were converted into percentage phosphorylation using the uninhibited (DMSO-treated) cells as high (= 100%) control and cells treated with 10 μM Staurosporine as low (= 0%) control. IC_{50} values were determined using the program GraphPad Prism 5 (GraphPad Software, Inc., La Jolla, CA), assuming a sigmoidal dose response.

Endothelial Cell Sprouting in the Spheroid-Based Cellular Angiogenesis Assay. The experiments were pursued in modification of the originally published protocol.[42] Primary human umbilical vein endothelial cells (HUVEC, PromoCell, Heidelberg, Germany) were used in endothelial cell growth and basal medium (ECGM/ECBM, PromoCell). In brief, spheroids were prepared as described[43] by pipetting 500 ECs (endothelial cells) in a hanging drop on plastic dishes to allow overnight spheroid aggregation. Then 50 EC spheroids were seeded in 0.9 mL of a collagen solution and pipetted into individual wells of a 24-well plate to allow polymerization. The test compounds in combination with VEGF-A [25 ng/mL final assay concentration] were added after 30 min by pipetting 100 μL of a 10-fold concentrated working dilution on top of the polymerized gel. Plates were incubated at 37 °C for 24 h and fixed by adding 4% paraformaldehyde. Sprouting intensity of ECs was quantitated by an image analysis system determining the cumulative sprout length per spheroid using an inverted microscope and the digital imaging software Analysis 3.2 (Soft imaging system, Münster, Germany). The mean of the cumulative sprout length of 10 randomly selected spheroids was analyzed as an individual data point. Fitting of IC_{50} curves and calculation of IC_{50} values was performed with GraphPad Prism 5.01 (GraphPad Software, Inc., La Jolla, CA).

In Vitro Cell Line Screening. The in vitro cell line screening was performed at the American National Cancer Institute (Bethesda, MD).[36] In brief, 60 human tumor cell lines were cultivated in RPMI 1640 medium containing 5% fetal bovine serum and 2 mM L-glutamine. Cells were inoculated into 96-well microtiter plates with plating densities ranging from 5000 to 40000 cells/well and were then incubated at 37 °C, 5% CO_2, 95% air, and 100% relative humidity for 24 h. After 24 h, representatives of cell lines are fixed with TCA to determine the cell density at the time of drug addition (Tz). Stock solutions of test compounds in DMSO (400-fold of the final maximum test concentration) were diluted with growth medium containing 50 μg/mL gentamicin to provide five drug concentrations. Then 100 μL aliquots of these test compound dilutions were added to the microtiter wells already containing the cancer cells and 100 μL of medium. The plates were incubated for 48 h at 37 °C, 5% CO_2, 95% air, and 100% relative humidity. Cells were fixed in situ by addition of 50 μL of cold 50% (w/v) TCA and incubated for 60 min at 4 °C. After discarding the supernatant, the plates were washed five times with water and air-dried. Then 100 μL of 0.4% sulforhodamine B (SRB) solution in 1% acetic acid was added. After 10 min, the cavities are washed five times with 1% acetic acid and the plates were air-dried. Bound SRB is solubilized with 10 mM trizma base, and the absorbance at 515 nm was measured on a plate reader. The percentage of growth is calculated at each of the five concentrations levels. Using the different absorbance measurements [time zero, (Tz), control growth, (C), and growth in the presence of drug (Ti)], the growth inhibition 50% (GI_{50}) is the concentration for a Ti value satisfying the equation $[(Ti - Tz)/(C - Tz)] \times 100 = 50$.

Compounds were initially evaluated in a prescreening at a single dose of 10 μM against the 60 human cancer cell lines. Only those structures which show a considerable antiproliferative activity in the prescreening were subsequently tested at five concentration levels for determination of GI_{50} values. Further details of the test method have been published.[33,34,44]

Docking. For a selection of kinase structures suitable for the docking, high-resolution crystal structures ranging from 1.65 to 2.1 Å were retrieved from the PDB. Subsequently, the most "CDK2-like" PDB files of the respective protein kinases were searched because the paullones, the archetype of the docked prototypes A−D, interact best with cyclin dependent kinases. The CDK2-likeness was analyzed by aligning the structures to the phosphorylated CDK2/magnesium ATP complex structure (PDB code 1QMZ) as a common reference by superimposing the Cα-backbone atoms of 38 residues able to interact with ATP-competitive inhibitors using singular value decomposition, which allows superimposition of all ligands in a common framework.[45] The rms deviations for the pairwise superimposed ATP binding pockets were calculated and act as indicator for the active-state CDK2-likeness. The structures selected based on this rationale were 1YWN (for VEGF-R2), 2OWB (for PLK1), and 3BU6 (for INS-R).

The docking calculations were performed using the Schrödinger software suite with default settings if not indicated otherwise. For protein preparation, all the crystallographic water molecules were removed, hydrogens were added, and bond orders were assigned using Maestro's Protein Preparation Wizard (Maestro v. 8.5207).[46] The added hydrogen atoms were minimized with all heavy atoms fixed using the OPLS2001 force field. For each of the three structures, energy grids were built using the default value of protein atom scaling within a cubic box of dimensions 28 Å × 28 Å × 28 Å. This box was centered around the centroid of the ATP bound to/from the common reference 1QMZ. The bounding box dimensions, inside which the centroid of a docked pose was restricted, were set to 16 Å × 16 Å × 16 Å.

Docking was performed using Schödingers Glide.[47−49] To attain a variety of docking poses, a first run was performed using the standard-precision (SP) mode with a scaling factor for the van der Waals radii scaling of 0.7. The obtained poses were refined using Glide's extra-precision mode (XP, Impact v. 5.0207) with default settings.

Hotspot Analysis. GRID computations were carried out using version 22a.[50] Hydrogens were added with the program GRIN (part of the GRID package). The grid spacing was set to 0.33 Å; all other GRID input parameters retained their default values.

Synthetic Chemistry. Monomode microwave device: CEM Discover focused microwave synthesis system with ChemDriver software. Melting points (mp) were determined on an electric variable heater (Barnstead Electrothermal IA 9100) and were not corrected. IR spectra were recorded as KBr discs on a Thermo Nicolet FT-IR 200. ^{1}H NMR spectra and ^{13}C NMR spectra were recorded on the following instruments: Bruker Avance DRX-400 and Bruker Avance II-600, solvent DMSO-d_6 if not stated otherwise, internal standard trimethylsilane, signals in ppm (δ scale). Elemental analyses were determined on a CE Instruments FlashEA 1112 elemental analyzer (Thermo Quest). Mass spectra were recorded on a double-focused sector field

mass spectrometer Finnigan-MAT 90. Accurate measurements where conducted according to the peakmatch method using perfluorokerosene (PFK) as an internal mass reference; (EI)-MS: ionization energy 70 eV. TLC: Polygram Sil G/UV_{254}, Macherey-Nagel, 40 mm × 80 mm, visualization by UV illumination (254 nm). Column chromatography: silica gel 60 (Merck), column width 2 cm, column height 10 cm unless stated otherwise. Purity was determined by HPLC using the following devices and settings: Elite LaChrom (Merck/Hitachi), pump L-2130, autosampler L-2200, diode array detector L-2450, organizer box L-2000; column: Merck LiChroCART 125-4, LiChrosphere 100, RP 18, 5 μm, flow rate 1.000 mL/min, isocratic, volume of injection 10 μL; detection (DAD) at 254 and 280 nm; AUC % method; time of detection 15 min, net retention time (t_N), dead time (t_m) related to DMSO. Preparation of H_2O + $(Et_3NH)_2SO_4$-buffer (pH 2.5) for HPLC: triethylamine (20.0 mL) and sodium hydroxide (242 mg) were dissolved in water (980 mL). The solution was adjusted to pH 2.5 by addition of sulfuric acid. Preparation of H_2O/TFA mixture pH 1.5 for HPLC: water was adjusted to pH 1.5 by addition of TFA. All compounds employed in biological tests were used in ≥95% purity. The following compounds were prepared according to literature methods: **5**,[30] **6**,[31] **7**,[28] **8**,[27] **9**,[32] **16**.[51] Compounds **13**, **14**, **15** were purchased from commercial suppliers and were used without further purification. Synthetic procedures for the following compounds are available in the Supporting Information: **11**, **12**, **17a−b**, **18a−b**, **19**, **20a−b**, **21**, **22**, **23**, **24a−b**, **25a−b**, **26a−b, 27a−b, 28a−p, 29c, 29g, 29j, 29n, 30c**, **30g**, **30i**, **30j**, **30o**, **31c, 31 g, 31i, 31j, 31o.**

General Procedure A for the Preparation of Enaminones 10, 11, 12. A slurry of the respective azepinedione **6**, **7**, or **8** (1.00 mmol) in DMF-DMA (3.50 mL, 26.0 mmol) was stirred at 115−120 °C for 2.5 h. After cooling to room temperature, the resulting precipitate was collected, washed with petrolether, and crystallized from ethanol.

4-[(Dimethylamino)methylidene]-8-methoxy-3,4-dihydro-1*H*-1-benzazepine-2,5-dione (10). Preparation according to general procedure A yielded yellow crystals (73%); mp 245 °C. IR (KBr): 3174 cm^{-1} (NH), 1684 cm^{-1} and 1633 cm^{-1} (C=O). ^{1}H NMR ($CHCl_3$-d_1, 400 MHz): δ (ppm) = 3.26 (s, 6H, $-N(CH_3)_2$), 3.83 (s, 3H, $-OCH_3$), 3.42 (s, 2H, CH_2), 6.40 (d, 1H, J = 2.4 Hz, ar H), 6.77 (dd, 1H, J = 8.8/2.5 Hz, ar H), 7.74 (s, 1H, C=H), 7.88 (s, 1H, NH), 7.93 (d, 1H, J = 8.9 Hz, ar. H). Anal. ($C_{14}H_{16}N_2O_3$) C, H, N. HPLC (ACN:H_2O 20:80): purity 100.0% at 254 nm, 100.0% at 280 nm; t_N 2.73 min; t_m(DMSO) 1.03 min.

General Procedure B for the Synthesis of 2-Anilino-5,7-dihydro-6*H*-pyrimido[5,4-*d*][1]benzazepin-6-ones 28 and 29 and the Analogues 30 and 31. Method 1. The enaminone **9**, **10**, **11**, or **12** (1.00 mmol) was refluxed with the respective arylguanidinium nitrate **16** (1.2 mmol) and NaOH (48 mg, 1.2 mmol) in propan-2-ol (5 mL) for the indicated reaction time. After cooling to room temperature, the resulting precipitate was collected and successively washed with water and petrolether.

Method 2. The enaminone **9** (1.00 mmol) was reacted with the respective arylguanidinium nitrate **16** (1.2 mmol) and NaOH (48 mg, 1.2 mmol) in propan-2-ol (5 mL). The reaction was conducted in a microwave device using a sealed microwave reaction vessel for 30−40 min at 150 °C. After cooling to room temperature, the resulting precipitate was collected and successively washed with water and petrolether.

2-(4-Ethoxyanilino)-9-methoxy-5,7-dihydro-6*H*-pyrimido[5,4-*d*]-[1]benzazepin-6-one (29i). Preparation according to general procedure B, method 1 from **10** (reaction time 15 h). Crystallization from EtOH yielded 74% colorless crystals; mp 267 °C. IR (KBr): 3257 cm^{-1} and 3196 cm^{-1} (NH), 1680 cm^{-1} (C=O). ^{1}H NMR (DMSO-d_6, 400 MHz): δ (ppm) = 1.31 (t, 3H, J = 7.0 Hz, $-OCH_2CH_3$), 3.33 (s, 2H, CH_2; superimposed by H_2O peak), 3.83 (s, 3H, $-OCH_3$), 3.98 (q, 2H, J = 7.1 Hz, $-OCH_2CH_3$), 6.76 (d, 1H, J = 2.3 Hz, ar H), 6.84−6.88 (m, 2H, ar H), 6.95 (dd, 1H, J = 8.5/2.6 Hz, ar H), 7.65−7.69 (m, 2H, ar H), 8.00 (d, 1H, J = 8.8 Hz, ar H), 8.39 (s, 1H, pyrimidine-H), 9.45 (s, 1H, NH), 10.14 (s, 1H, NH). Anal. ($C_{21}H_{20}N_4O_3$) C, H, N. HPLC (ACN:H_2O 50:50): purity 96.3% at 254 nm, 97.8% at 280 nm; t_N 2.92 min; t_m(DMSO) 1.03 min.

2-(3-Chloro-4-hydroxyanilino)-9-methoxy-5,7-dihydro-6*H*-pyrimido[5,4-*d*][1]benzazepin-6-one (29o). Preparation according to general procedure B, method 1 (reaction time 24 h). Crystallization from EtOH yielded 35% beige crystals; mp 275 °C. IR (KBr): 3185 cm^{-1} (NH), ca. 2800−3200 (OH), 1655 cm^{-1} (C=O). ^{1}H NMR (DMSO-d_6, 400 MHz): δ (ppm) = 3.35 (s, 2H, CH_2 superimposed by H_2O peak), 3.84 (s, 3H, $-OCH_3$), 6.78 (d, 1H, J = 2.6 Hz, ar H), 6.91 (d, 1H, J = 8.8, ar H), 6.96 (dd, 1H, J = 8.7/2.5 Hz, ar H), 7.50 (dd, 1H, J = 8.9/2.6, ar H), 7.90 (d, 1H, J = 2.6 Hz, ar H), 8.00 (d, 1H, J = 8.8 Hz, ar H), 8.42 (s, 1H, pyrimidine-H), 9.52 (s, 1H, NH), 9.68 (s, 1H, OH), 10.16 (s, 1H, NH). ($C_{19}H_{15}ClN_4O_3$) HRMS (EI) (m/z): $[M - H]^+$ calcd 381.07544, found 381.07470. HPLC (ACN:H_2O 35:65): purity: 98.4% at 254 nm, 98.4% at 280 nm; t_N 3.84 min, t_m (DMSO) 1.03 min.

Acknowledgment. We are grateful to the National Cancer Institute for performing the in vitro cell line screening. The work was funded in part by the European Commission (contract no. LSHB-CT-2004-503467, to A.-M. E.-S., U. D., H. W., J.E.E., B. M., F. T., C. S., M. H. G. K., and C. K.) and the Deutsche Forschungsgemeinschaft (DFG, to J. D. and K. B.).

Supporting Information Available: Two-dimensional sketches of the docking results for **1**, **21**, **24a**, and **28a** in VEGF-R2, PLK1, and INS-R, respectively; ^{13}C NMR data of **10**, **29i**, and **29o**; details for the synthesis, spectroscopic data, and HPLC purity data of **11**, **12**, **17a−b**, **18a−b**, **19**, **20a−b**, **21**, **22**, **23**, **24a−b, 25a−b, 26a−b, 27a−b, 28a−p, 29c, 29g, 29j, 29n, 30c, 30g, 30i, 30j, 30o, 31c, 31g, 31i, 31j,** and **31o**. This material is available free of charge via the Internet at http://pubs.acs.org.

References

(1) Arora, A.; Scholar, E. Role of tyrosine kinase inhibitors in cancer therapy. *J. Pharmacol. Exp. Ther.* **2005**, *315*, 971–979.
(2) Kunick, C.; Egert-Schmidt, A. The short history of protein kinase inhibitors. New, competitive, successful. *Pharm. Unserer Z.* **2008**, *37*, 360–368.
(3) Zhang, J.; Yang, P.; Gray, N. Targeting cancer with small molecule kinase inhibitors. *Nat. Rev. Cancer* **2009**, *9*, 28–39.
(4) Spicer, J.; Rewcastle, G.; Kaufman, M.; Black, S.; Plummer, M.; Denny, W.; Quin, J. r.; Shahripour, A.; Barrett, S.; Whitehead, C.; Milbank, J.; Ohren, J.; Gowan, R.; Omer, C.; Camp, H.; Esmaeil, N.; Moore, K.; Sebolt-Leopold, J. P. S; Merriman, R.; Ortwine, D.; Warmus, J.; Flamme, C.; Pavlovsky, A.; Tecle, H. 4-Anilino-5-carboxamido-2-pyridone derivatives as noncompetitive inhibitors of mitogen-activated protein kinase kinase. *J. Med. Chem.* **2007**, *50*, 5090–5102.
(5) Petrelli, A.; Giordano, S. From single- to multi-target drugs in cancer therapy: when aspecificity becomes an advantage. *Curr. Med. Chem.* **2008**, *15*, 422–432.
(6) Mendel, D. B.; Laird, A. D.; Xin, X.; Louie, S. G.; Christensen, J. G.; Li, G.; Schreck, R. E.; Abrams, T. J.; Ngai, T. J.; Lee, L. B.; Murray, L. J.; Carver, J.; Chan, E.; Moss, K. G.; Haznedar, J. O.; Sukbuntherng, J.; Blake, R. A.; Sun, L.; Tang, C.; Miller, T.; Shirazian, S.; McMahon, G.; Cherrington, J. M. In vivo antitumor activity of SU11248, a novel tyrosine kinase inhibitor targeting vascular endothelial growth factor and platelet-derived growth factor receptors: Determination of a pharmacokinetic/pharmacodynamic relationship. *Clin. Cancer Res.* **2003**, *9*, 327–337.
(7) Wilhelm, S.; Carter, C.; Lynch, M.; Lowinger, T.; Dumas, J.; Smith, R.; Schwartz, B.; Simantov, R.; Kelley, S. Discovery and development of sorafenib: a multikinase inhibitor for treating cancer. *Nat. Rev. Drug Discovery* **2006**, *5*, 835–844.
(8) Carter, T.; Wodicka, L.; Shah, N.; Velasc, A.; Fabian, M.; Treiber, D.; Milanov, Z.; Atteridge, C.; Biggs, W. r.; Edeen, P.; Floyd, M.; Ford, J.; Grotzfeld, R.; Herrgard, S.; Insko, D.; Mehta, S.; Patel, H.; Pao, W.; Sawyers, C.; Varmus, H.; Zarrinkar, P.; Lockhart, D. Inhibition of drug-resistant mutants of ABL, KIT, and EGF

receptor kinases. *Proc. Natl. Acad. Sci. U.S.A.* **2005**, *102*, 11011–11016.
(9) Shah, N.; Tran, C.; Lee, F.; Chen, P.; Norris, D.; Sawyers, C. Overriding imatinib resistance with a novel ABL kinase inhibitor. *Science* **2004**, *305*, 399–401.
(10) Petronczki, M.; Lénárt, P.; Peters, J. Polo on the rise-from mitotic entry to cytokinesis with PLK1. *Dev. Cell* **2008**, *14*, 646–659.
(11) Strebhardt, K.; Ullrich, A. Targeting polo-like kinase 1 for cancer therapy. *Nat. Rev. Cancer* **2006**, *6*, 321–330.
(12) Spänkuch-Schmitt, B.; Bereiter-Hahn, J.; Kaufmann, M.; Strebhardt, K. Effect of RNA silencing of polo-like kinase-1 (PLK1) on apoptosis and spindle formation in human cancer cells. *J. Natl. Cancer Inst.* **2002**, *94*, 1863–1877.
(13) Spänkuch-Schmitt, B.; Wolf, G.; Solbach, C.; Loibl, S.; Knecht, R.; Stegmüller, M.; von Minckwitz, G.; Kaufmann, M.; Strebhardt, K. Downregulation of human polo-like kinase activity by antisense oligonucleotides induces growth inhibition in cancer cells. *Oncogene* **2002**, *21*, 3162–3171.
(14) Spänkuch, B.; Matthess, Y.; Knecht, R.; Zimmer, B.; Kaufmann, M.; Strebhardt, K. Cancer inhibition in nude mice after systemic application of U6 promoter-driven short hairpin RNAs against PLK1. *J. Natl. Cancer Inst.* **2004**, *96*, 862–872.
(15) Steegmaier, M.; Hoffmann, M.; Baum, A.; Lénárt, P.; Petronczki, M.; Krssák, M.; Gürtler, U.; Garin-Chesa, P.; Lieb, S.; Quant, J.; Grauert, M.; Adolf, G.; Kraut, N.; Peters, J.; Rettig, W. BI 2536, a potent and selective inhibitor of polo-like kinase 1, inhibits tumor growth in vivo. *Curr. Biol.* **2007**, *17*, 316–322.
(16) McIntyre, J. Sunitinib malate. *Drugs Future* **2005**, *30*, 785–792.
(17) Press, M.; Lenz, H. EGFR, HER2 and VEGF pathways: validated targets for cancer treatment. *Drugs* **2007**, *67*, 2045–2075.
(18) Folkman, J. What is the evidence that tumors are angiogenesis dependent? *J. Natl. Cancer Inst.* **1990**, *82*, 4–6.
(19) Gilbert, M.; Mousa, S.; Mousa, S. Current status of anti-vascular endothelial growth factor (VEGF) stategies and future directions. *Drugs Fut.* **2008**, *33*, 515–525.
(20) Underiner, T.; Ruggeri, B.; Gingrich, D. Development of vascular endothelial growth factor receptor (VEGFR) kinase inhibitors as anti-angiogenic agents in cancer therapy. *Curr. Med. Chem.* **2004**, *11*, 731–745.
(21) Zhong, H.; Bowen, J. Molecular design and clinical development of VEGFR kinase inhibitors. *Curr. Top. Med. Chem.* **2007**, *7*, 379–393.
(22) Ghose, A.; Herbertz, T.; Pippin, D.; Salvino, J.; Mallamo, J. Knowledge based prediction of ligand binding modes and rational inhibitor design for kinase drug discovery. *J. Med. Chem.* **2008**, *51*, 5149–5171.
(23) Pies, T.; Schaper, K.-J.; Leost, M.; Zaharevitz, D. W.; Gussio, R.; Meijer, L.; Kunick, C. CDK1-inhibitory activity of paullones depends on electronic properties of 9-substituents. *Arch. Pharm. Pharm. Med. Chem.* **2004**, *337*, 486–492.
(24) Leost, M.; Schultz, C.; Link, A.; Wu, Y.-Z.; Biernat, J.; Mandelkow, E.-M.; Bibb, J. A.; Snyder, G. L.; Greengard, P.; Zaharevitz, D. W.; Gussio, R.; Senderowicz, A. M.; Sausville, E. A.; Kunick, C.; Meijer, L. Paullones are potent inhibitors of glycogen synthase kinase-3b and cyclin-dependent kinase 5/p25. *Eur. J. Biochem.* **2000**, *267*, 5983–5994.
(25) Lahusen, T.; De Siervi, A.; Kunick, C.; Senderowicz, A. Alsterpaullone, a novel cyclin-dependent kinase inhibitor, induces apoptosis by activation of caspase 9 due to perturbation in mitochondrial membrane potential. *Mol. Carcinog.* **2003**, *36*, 183–194.
(26) Bertrand, J. A.; Thieffine, S.; Vulpetti, A.; Cristiani, C.; Valsasina, B.; Knapp, S.; Kalisz, H. M.; Flocco, M. Structural characterization of the GSK-3beta active site using selective and non-selective ATP-mimetic inhibitors. *J. Mol. Biol.* **2003**, *333*, 393–407.
(27) Kunick, C.; Lauenroth, K.; Leost, M.; Meijer, L.; Lemcke, T. 1-Azakenpaullone is a selective inhibitor of glycogen synthase kinase-3. *Bioorg. Med. Chem. Lett.* **2004**, *14*, 413–416.
(28) Stukenbrock, H.; Mussmann, R.; Geese, M.; Ferandin, Y.; Lozach, O.; Lemcke, T.; Kegel, S.; Lomow, A.; Burk, U.; Dohrmann, C.; Meijer, L.; Austen, M.; Kunick, C. 9-Cyano-1-azapaullone (cazpaullone), a glycogen synthase kinase-3 (GSK-3) inhibitor activating pancreatic beta cell protection and replication. *J. Med. Chem.* **2008**, *51*, 2196–2207.
(29) Bain, J.; Plater, L.; Elliott, M.; Shpiro, N.; Hastie, C.; McLauchlan, H.; Klevernic, I.; Arthur, J.; Alessi, D.; Cohen, P. The selectivity of protein kinase inhibitors: a further update. *Biochem. J.* **2007**, *408*, 297–315.
(30) Kunick, C. Synthese [*b*]-kondensierter Azepindione durch Dealkoxycarbonylierung. *Arch. Pharm.* (*Weinheim*) **1991**, *324*, 579–581.
(31) Wieking, K.; Knockaert, M.; Leost, M.; Zaharevitz, D. W.; Meijer, L.; Kunick, C. Synthesis of paullones with aminoalkyl side chains. *Arch. Pharm. Pharm. Med. Chem.* **2002**, *335*, 311–317.
(32) Chen, W.-Y.; Gilman, N. W. Synthesis of 7-phenylpyrimido[5,4-*d*][1]benzazepin-2-ones. *J. Heterocycl. Chem.* **1983**, *20*, 663–666.
(33) Shoemaker, R. The NCI60 human tumour cell line anticancer drug screen. *Nat. Rev. Cancer* **2006**, *6*, 813–823.
(34) Boyd, M. R.; Paull, K. D. Some practical considerations and applications of the National Cancer Institute in vitro anticancer drug discovery screen. *Drug Dev. Res.* **1995**, *34*, 91–109.
(35) Paull, K. D.; Shoemaker, R. H.; Hodes, L.; Monks, A.; Scudiero, D. A.; Rubinstein, L.; Plowman, J.; Boyd, M. R. Display and analysis of patterns of differential activity of drugs against human tumor cell lines: development of meangraph and COMPARE algorithm. *J. Natl. Cancer Inst.* **1989**, *81*, 1088–1092.
(36) *NCI-60 DTP Human Tumor Cell Line Screen*; Developmental Therapeutics Program NCI/NIH; http://dtp.nci.nih.gov/branches/btb/ivclsp.html (accessed **2008**).
(37) Andreani, A.; Burnelli, S.; Granaiola, M.; Leoni, A.; Locatelli, A.; Morigi, R.; Rambaldi, M.; Varoli, L.; Landi, L.; Prata, C.; Berridge, M.; Grasso, C.; Fiebig, H.; Kelter, G.; Burger, A.; Kunkel, M. Antitumor activity of bis-indole derivatives. *J. Med. Chem.* **2008**, *51*, 4563–4570.
(38) Kunick, C.; Bleeker, C.; Prühs, C.; Totzke, F.; Schächtele, C.; Kubbutat, M. H. G.; Link, A. Matrix compare analysis discriminates subtle structural differences in a family of novel antiproliferative agents, diaryl-3-hydroxy-2,3,3a,10a-tetrahydrobenzo[*b*]-cylopenta[*e*]azepine-4,10(1*H*,5*H*)-diones. *Bioorg. Med. Chem. Lett.* **2006**, *16*, 2148–2153.
(39) Goodford, P. J. A computational procedure for determining energetically favorable binding sites on biologically important macromolecules. *J. Med. Chem.* **1985**, *28*, 849–857.
(40) Blackburn, C.; Claiborne, C. F.; Cullis, C. A.; Dales, N. A.; Patane, M. A.; Stirling, M.; Stradella, O. G.; Weatherhead, G. S. Preparation of lactam compounds useful as protein kinase inhibitors. Patent WO 2006041773, **2006**.
(41) Zhang, J.; Chung, T.; Oldenburg, K. A simple statistical parameter for use in evaluation and validation of high throughput screening assays. *J. Biomol. Screening* **1999**, *4*, 67–73.
(42) Korff, T.; Augustin, H. Tensional forces in fibrillar extracellular matrices control directional capillary sprouting. *J. Cell Sci.* **1999**, *112*, 3249–3258.
(43) Korff, T.; Augustin, H. Integration of endothelial cells in multicellular spheroids prevents apoptosis and induces differentiation. *J. Cell Biol.* **1998**, *143*, 1341–1352.
(44) Grever, M. R.; Schepartz, S. A.; Chabner, B. A. The National Cancer Institute: cancer drug discovery and development program. *Semin. Oncol.* **1992**, *19*, 622–638.
(45) Vulpetti, A.; Bosotti, R. Sequence and structural analysis of kinase ATP pocket residues. *Farmaco* **2004**, *59*, 759–765.
(46) *Maestro, version 8.5*; Schrödinger, L.L.C.: New York, 2008.
(47) *Glide, version 5.0*; Schrödinger, L.L.C.: New York, 2008.
(48) Friesner, R. A.; Banks, J. L.; Murphy, R. B.; Halgren, T. A.; Klicic, J. J.; Mainz, D. T.; Repasky, M. P.; Knoll, E. H.; Shelley, M.; Perry, J. K.; Shaw, D. E.; Francis, P.; Shenkin, P. S. Glide: a new approach for rapid, accurate docking and scoring. 1. Method and assessment of docking accuracy. *J. Med. Chem.* **2004**, *47*, 1739–1749.
(49) Halgren, T. A.; Murphy, R. B.; Friesner, R. A.; Beard, H. S.; Frye, L. L.; Pollard, W. T.; Banks, J. L. Glide: a new approach for rapid, accurate docking and scoring. 2. Enrichment factors in database screening. *J. Med. Chem.* **2004**, *47*, 1750–1759.
(50) *GRID version 22a*; Molecular Discovery Ltd.: Oxford, UK, 2004.
(51) Tavares, F.; Boucheron, J.; Dickerson, S.; Griffin, R.; Preugschat, F.; Thomson, S.; Wang, T.; Zhou, H. *N*-Phenyl-4-pyrazolo[1,5-*b*]pyridazin-3-ylpyrimidin-2-amines as potent and selective inhibitors of glycogen synthase kinase 3 with good cellular efficacy. *J. Med. Chem.* **2004**, *47*, 4716–4730.